Electronic Supplementary Information (ESI)

Electric-field-induced supramolecular phase transitions at the liquid/solid interface: Cat-assembly from solvent additives

Ayyaz Mahmood,[a,b] Xingming Zeng,[a] Awais Siddique Saleemi,[a,b] Kum-Yi Cheng,[a,b] and Shern-Long Lee[a,*]

[a] Institute for Advanced Study, Shenzhen University, Shenzhen, Guangdong, China 518060

[b] Key Laboratory of Optoelectronic Devices and Systems of Ministry of Education and Guangdong Provence, College of Optoelectronic Engineering, Shenzhen University, Shenzhen, Guangdong, China 518060

*To whom correspondence should be addressed: sllee@szu.edu.cn

Content

Experimental

STM experiments

The STM experiments were performed at the OA/HOPG interface using a Keysight 5500 operating in the sample-biased and constant-current mode at room temperature (ca. 22 °C). The experiments were repeated several times. STM tips were mechanically cut Pt/Ir wires (80%/20%, diameter 0.25 mm). HOPG was purchased from Advanced Ceramics (ZYB grade, Advanced Ceramics Inc.). Imaging conditions of E_{bias} and i_{set} were ranged from −1.50 to 1.50 V and from 80 to 150 pA, respectively. The reported STM images were calibrated by the unit-cell vectors of the underlying HOPG using an SPIP software (scanning probe image processor, Image Metrology ApS). In addition to DI water, the chemicals were commercially available and were used as received. TMA molecules were weighed and dissolved in OA and the sample concentrations are 0.1 mM. The modelled molecular packing structures were obtained using HyperChem™ Professional 7.5 program based on the lattice-structure parameters. First, a molecular model for a single molecule was built, and then this model was duplicated. We constructed the model of the entire monolayer via placing the molecules in accordance with the intermolecular distances and angles obtained from calibrated STM images. The imaging parameters are indicated in the figure caption: sample bias (E_{bias}) and tunneling current (i_{set}).

Simulation methods

DFT simulations were performed using the functional M062X[1] with 6-31g(d) basis set.[2] The simulations were performed using Gaussian09 program.[3] The additives effects were simulated using the polarizable continuum model (PCM)[4] and radii were derived from UAKS approach[5] as implemented in Gaussian09 program. The PCM used to simulate the solvent effect is an implicit continuum model which represent the solvent as a continuum (a continuous medium) rather than explicit (individual) solvent molecules. The method is used as implemented in Gaussian09 program with no further modifications. The reactants, transition states, and products structures were optimized and vibrational frequency calculations were performed to calculate the Gibbs free energy.

The electric field effect were simulated using the keyword "field" as implemented in Gaussian by optimizing the obtained stationary points (reactants, transition states and products). The field simulations were performed in Z-matrix coordinates to control the orientation of the molecules with respect to the applied electric field. The field value of 9.0×10^8 Vm^{-1} was

used as obtained by dividing the voltage applied (0.9 V) in our STM experiments with a distance between an STM tip and the substrate underneath (1.0 nm).[6] The activation energy barriers and free energies of the reactions were calculated using the equations $\Delta G^{\ddagger} = \Delta G_{TS} - \Delta G_{ReactC}$and $\Delta_r G = \Delta G_{ProdC} - \Delta G_{ReactC}$, respectively. Where ΔG_{TS}, ΔG_{ReactC} and ΔG_{ProdC} are the free energy changes of the transition state, reactant complex, and product complex, respectively.

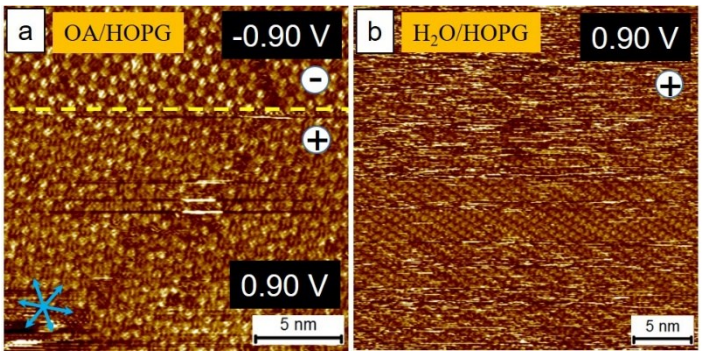

Fig. S1. STM images of the STM-polarity-related assemblies of TMA at the OA/HOPG and H_2O/HOPG. Imaging conditions (E_{bias}, $i_{tunneling}$) is ± 0.90 V, 100 pA. The results show that the chicken-wire motif of TMA can undergo phase transition at the H_2O/HOPG.

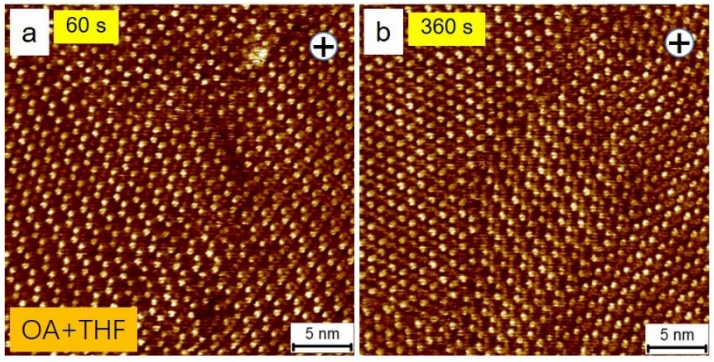

Fig. S2. STM images of the STM-polarity-related assemblies of TMA at the OA-THF/HOPG. Imaging conditions (E_{bias}, $i_{tunneling}$) is 0.90 V, 100 pA. The results show that the chicken-wire motif of TMA remains stable at least 5 minutes under positive STM bias at the OA-THF/HOPG.

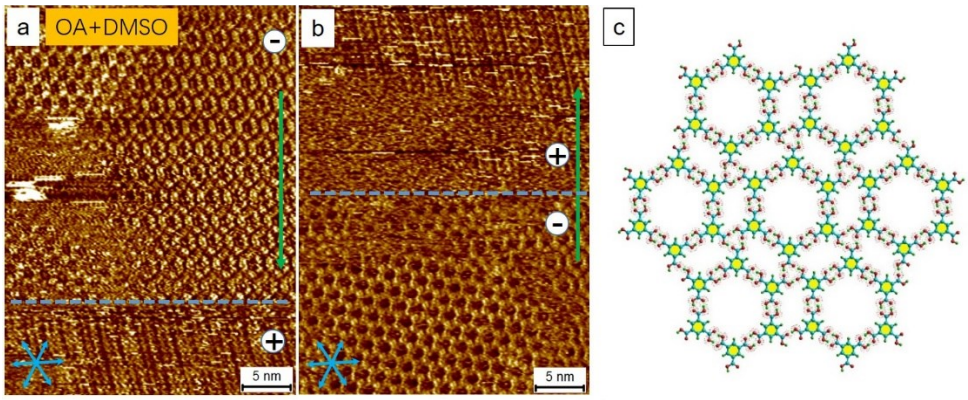

Fig. S3. STM images of the STM-polarity-related assemblies of TMA at the OA DMSO/HOPG. Imaging conditions (E_{bias}, $i_{tunneling}$) is ± 0.90 V, 100 pA. The results show that the chicken-wire and flower motifs of TMA can undergo phase transition at the OA DMSO/HOPG when the DMSO is 10%(v/v) in the OA-based sample solution.

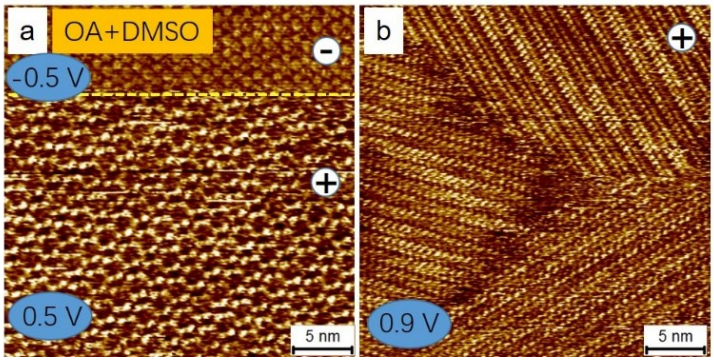

Fig. S4. STM image of the bias-related experiment of TMA assembly. The results show that if the substrate bias is changed from -0.5 V and maintained at 0.5 V first and tuned to 0.9V later, the chicken-wire motif can transfer to flower first and later transition to zigzag accordingly. Imaging conditions (E_{bias}, $i_{tunneling}$) is ± 0.5 V and 0.9 V, 100 pA.

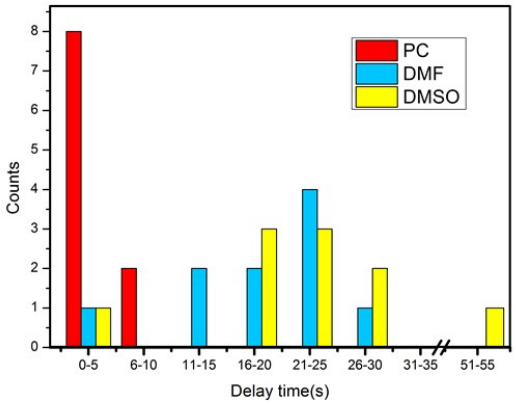

Fig. S5. A histogram of the delay time of phase transition after switching STM polarity from negative to positive. The delay time refers to the recorded time period by the phase transition to occur upon the change of STM polarity. The histogram represents the quantitative and qualitative analysis of the additives in the present system, suggesting a tendency that PC exhibits higher efficiency than DMF and DMSO for catalyzing the phase transitions triggered by STM. The concentrations of sample solutions are fixed to be the same (0.1 mM). The additives are 0.5 vol% for all the cases. The data was obtained by different tips and repeated by several experimental sections to avoid the difference resulting from the tip influence. The parameters of STM experiments are ±0.9V; 100 pA.

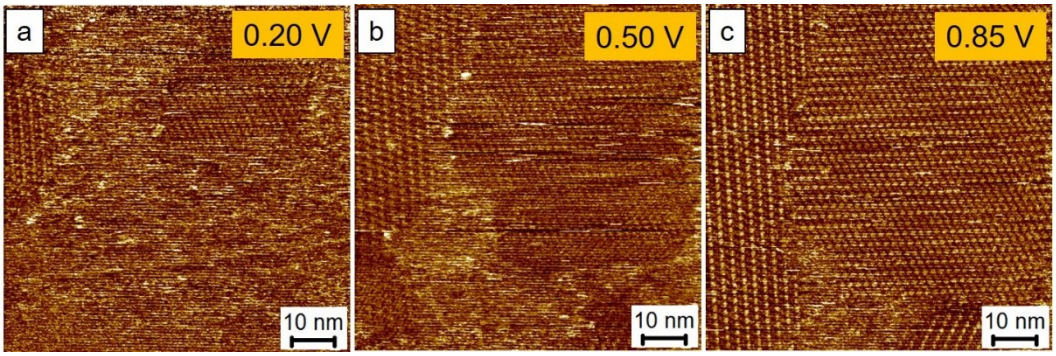

Fig. S6. STM images of the STM-bias-related assemblies of TMA at the H_2O/HOPG. Imaging conditions (E_{bias}, $i_{tunneling}$) are noted on the images, the tunneling current for all is 100 pA. The results show that unlike the PC, DMSO or DMF cases, the flower motif of TMA is absent using water as solvent.

Simulations

OA is always present at the interface while other additives (solvents) with a wide polarity range are added at the interface in the experiment to observe the additive effects on the phase transition of TMA. OA being an acid can release a proton and its conjugate base, C_7H_{15}-COO^-, can accept a proton from TMA to deprotonate it. It was previously proposed that OA has no role in the deprotonation of TMA and thus in its phase-transition. Although, the conjugate base of OA, C_7H_{15}-COO^-, in the presence of water has a small Gibbs reaction energy barrier (3.57 kcal mol^{-1})[7] for the proton transfer reaction from TMA to C_7H_{15}-COO^-, however, the barrier related to the deprotonation of OA to form its conjugate base is on the higher side, e.g., 7.77 kcal mol^{-1}.[7] Thus, we did not study this reaction in the present study because OA is always present at the interface (constant factor). Therefore, we studied the varying factor i.e. the additives. Moreover, note that TMA itself being a stronger acid than OA (pk_a: 3.12 *vs* 4.90) is expected to release a proton faster than OA to deprotonate itself.

The simulations are performed on single isolated TMA and solvent molecules. The effect of the electric field on the Gibbs activation and Free energies of reactions is also simulated. The activation and free energies of reactions are then compared to determine the solvent that causes the deprotonation of TMA with lowest activation energy. While a catalyst does not alter the global free energy, the free energies of deprotonation reactions of TMA by different solvents is different. By comparing these results, one can determine the thermochemistry (exo/endothermicity) of the reactions.

Table S1 and Fig. 4 present the calculated quantitative results of Gibbs activation and Free energies of the deprotonation reactions of TMA by different solvent molecules. The deprotonation reactions occurring at the interface has been suggested to be responsible for phase transition in literature. The solvent with lowest activation energy (PC) and lowest endothermicity will proceed the fastest partial deprotonation of TMA molecules at the interface which in turn will result in the phase transition. The solvents with higher activation energies are unable to cause an efficient, if any, deprotonation of TMA and hence no phase transition is observed for such solvents (acetone, methanol, THF).

Fig. S6 depicts the possible deprotonation reactions that can occur at the interface with PC additive. An efficient phase transition in the presence of PC can be due to the availability of multiple sites for the deprotonation reaction. Although reaction through PC-O^2 and PC-O^3 has a reasonably larger barriers for the deprotonation reaction, the overall rate (sum of three rates) of deprotonation of TMA is proposed to be larger, resulting in an efficient phase transition.

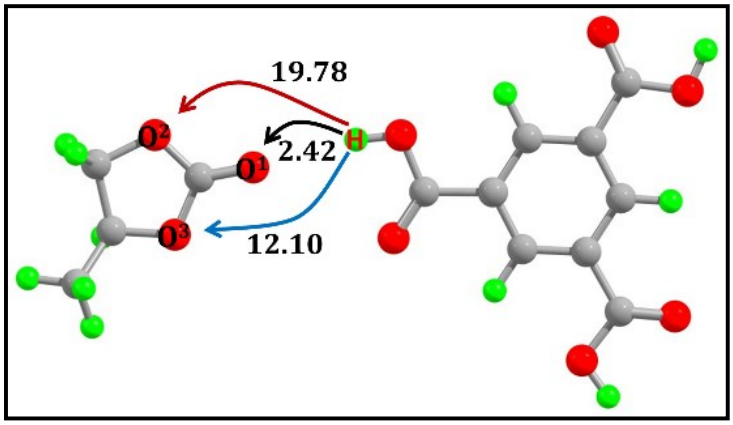

Fig. S7. The possible deprotonation reactions with PC additive along with Gibbs activation energy ($\Delta G^{\ddagger}$) values. Energy values in kcal mol^{-1}.

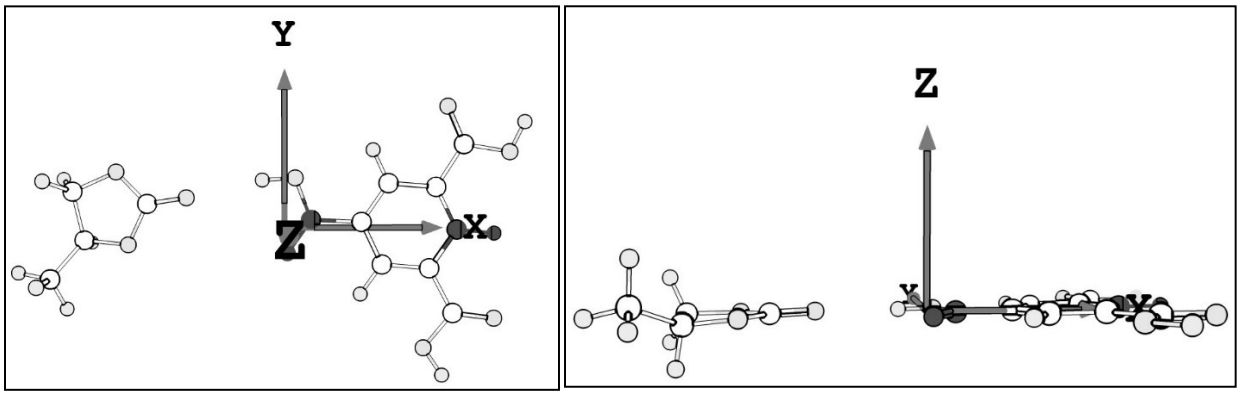

Fig. S8. The top (left) and side (right) view of the planes of TMA and PC with respect to the direction of the applied electric field in the simulations. The planes of optimized geometries of both the molecules are perpendicular to the direction of electric field and thus observing a great electric-field effect.

We used protonated models in Figure 2 in the manuscript. The partial deprotonation of TMA caused the negatively charged TMA molecules. However, the protons of the deprotonated molecules remain in the vicinity of the TMA molecules and move back and forth, as reported in literature. Therefore, the fully protonated models were presented in Figure 2 in the manuscript, likewise in literature where protonated models were reported although partial deprotonation may occur at the interface.[S7]

Table S1. The calculated Gibbs activation energies ($\Delta G^{\ddagger}$) and Gibbs reaction free energies ($^{\Delta_r G}$) for the deprotonation reaction of TMA caused by different additives, their dipole moments (Debye), dielectric constants (ε) and polarity index (PI). Energy values in kcal mol^{-1}. Simulated electric-field 0.9 V = 9.0 × 10^8 Vm^{-1} = V/d = 0.9 V/1 nm; where 1nm is the approximated the gap between the STM tip and the substrate.[S8] The calculations were performed with M062X functional using 6-31g(d) basis set.

Additive	$\Delta G^{\ddagger}$ (kcal mol^{-1})		$^{\Delta_r G}$ (kcal mol^{-1})		**μ** (Debye)		**ε**	**PI**
	EF = 0	EF = 0.9 V	EF = 0	EF = 0.9 V	Exp.[S9,S10]	DFT*		
PC-O[1]	13.31	2.42	24.81	5.84				
PC-O[2]	26.14	19.78	34.07	29.85	4.901	5.86	64.02	6.1
PC-O[3]	14.56	12.10	33.03	31.06				
DMSO	4.84	4.35	10.41	9.88	3.96	4.44	46.83	7.2
DMF	7.33	5.34	13.26	11.92	3.86	4.22	37.22	6.4
Methanol	12.41	11.53	30.54	21.19	1.69	1.89	32.61	5.1
Acetone	9.40	8.96	21.32	19.58	2.91	3.14	20.49	5.1
DCM	-	-	-	-	1.60	1.82	8.93	3.1
THF	10.11	9.65	21.10	20.04	1.63	1.99	7.43	4.0
Chloroform	-	-	-	-	1.15	1.20	4.71	2.7
Toluene	-	-	-	-	0.36	0.40	2.37	2.4

*Calculated with DFT/B3LYP/6-311++G(d,p).

The simulated deprotonation reactions

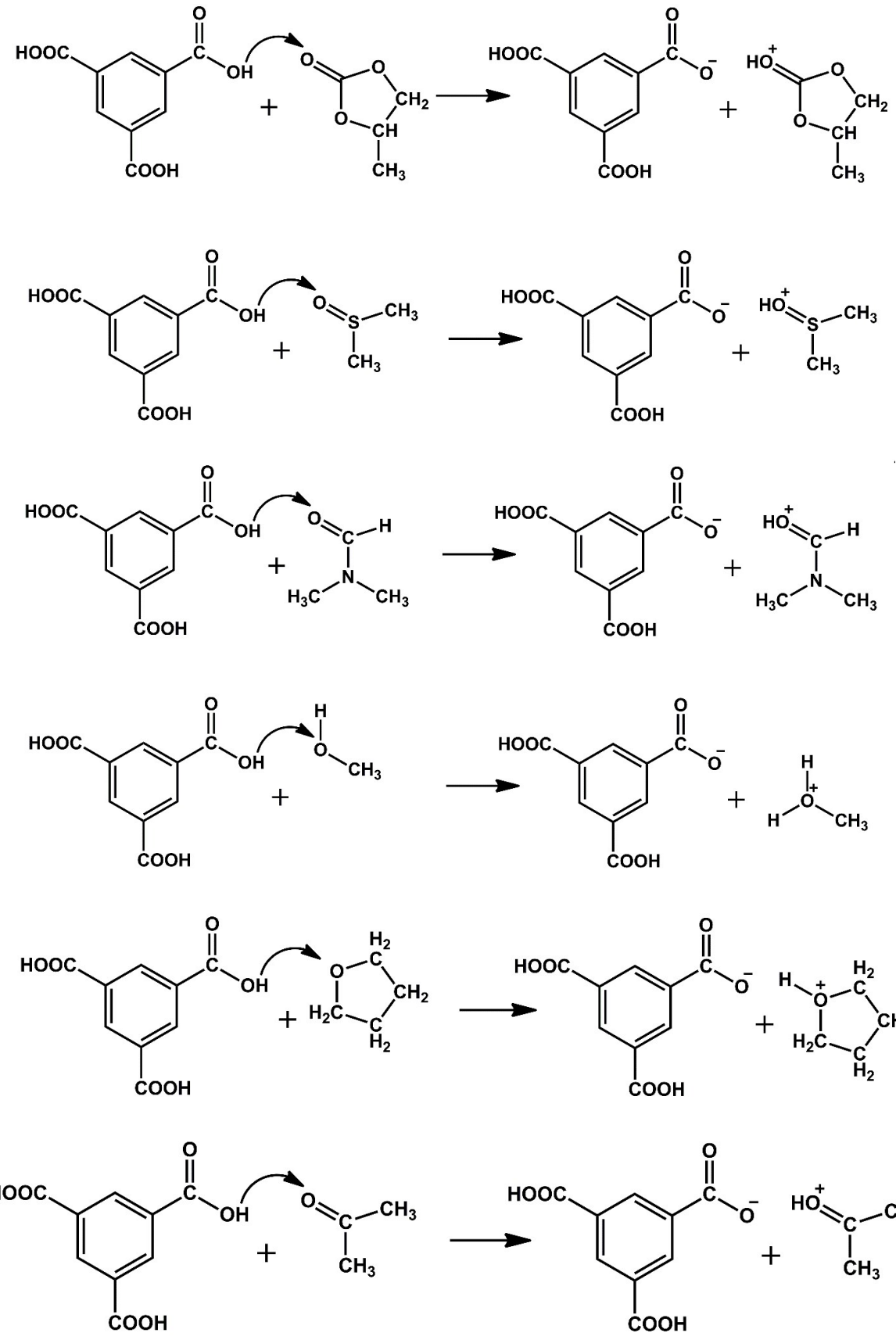

Scheme S1. The simulated deprotonation reactions of TMA occurring at the interface, resulting in the charged products.

Optimized geometries of stationary points (reactants, transition states and products).

Reactants	TSs	Products
TMA + PC		
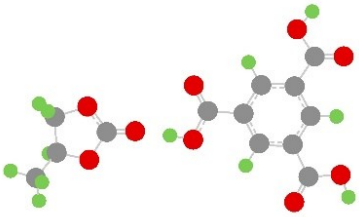	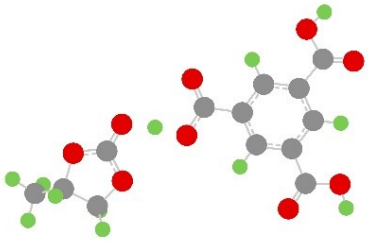	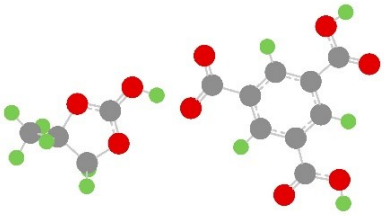
TMA+ DMSO		
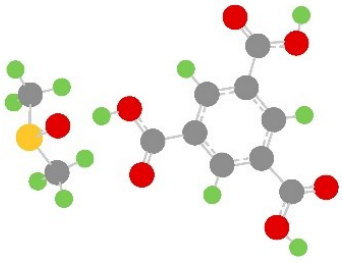	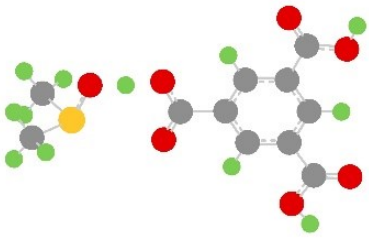	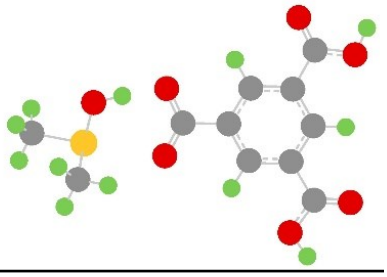
TMA + DMF		

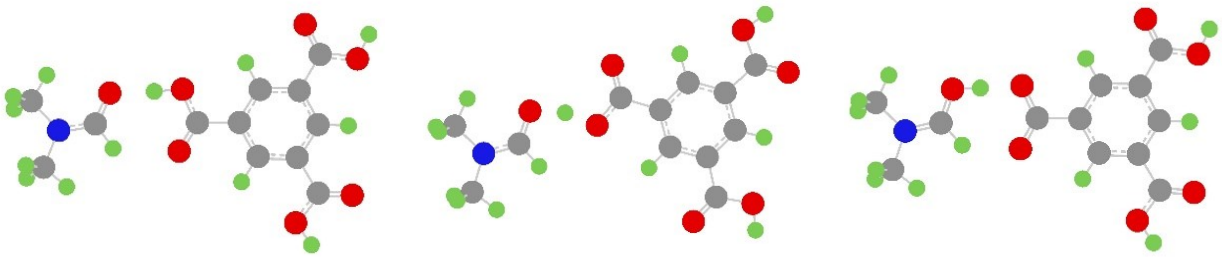

TMA + Methanol

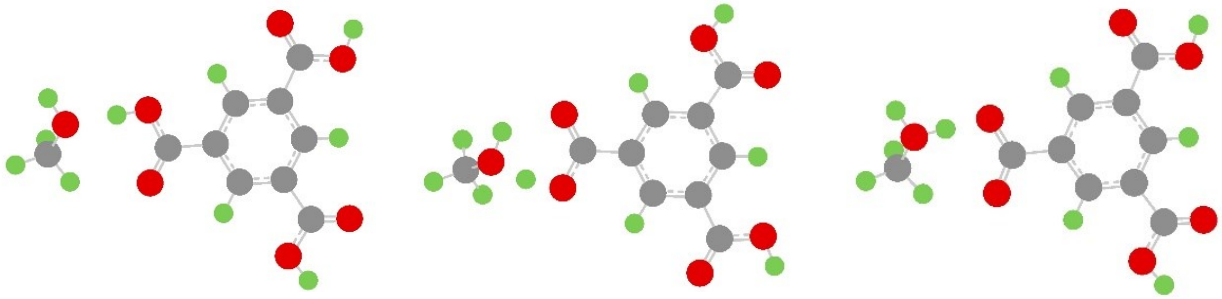

TMA + Acetone

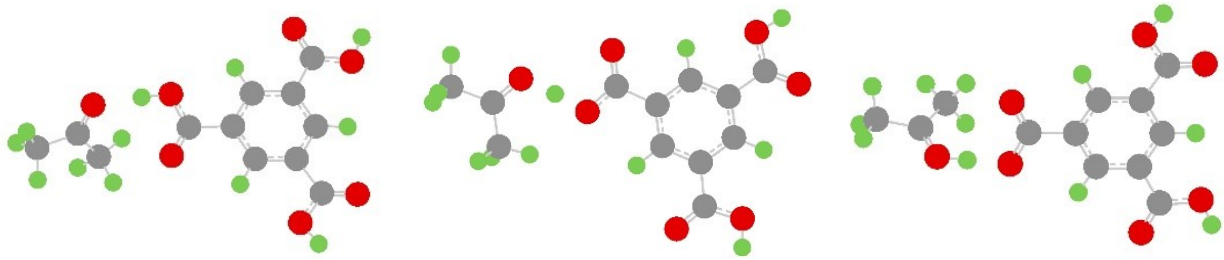

TMA + THF

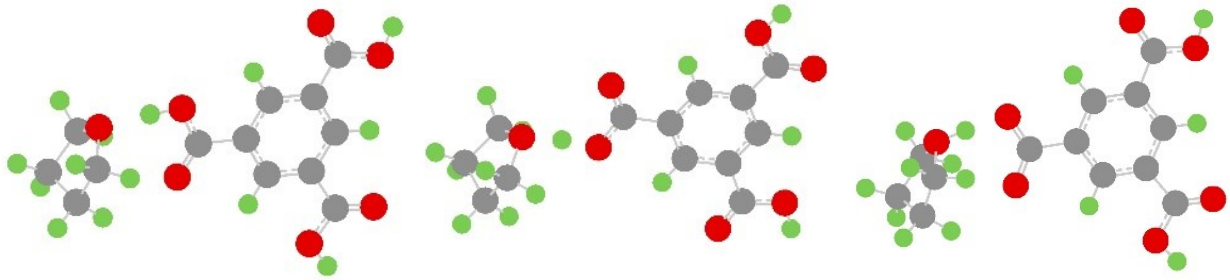

Gaussian input file for DMSO+TMA reactant complex structure.

```
%mem=32GB
%nprocshared=24
# opt freq 6-31g(d) scrf=(solvent=dmso,pcm)  m062x

C             0.00000000    0.00000000    0.00000000
 C            0.00000000    0.00000000    1.39431739
 C            1.20761673    0.00000000    2.08941774
 C            2.41738384   -0.00156375    1.39534432
 C            2.41339334   -0.00188783    0.00272221
 C            1.20577600   -0.00040510   -0.69629066
 H           -0.94683904   -0.00049832    1.92312401
 H            3.34971366   -0.00290413    1.94926341
 H            1.21546417   -0.00020367   -1.78076746
 C            3.67782677   -0.00583144   -0.78698883
 O            3.72135717   -0.01578259   -1.99587537
 O            4.77143166    0.00214058   -0.01470685
 H            5.54891511   -0.00202968   -0.60191415
 C            1.26012867   -0.00010049    3.57937999
 O            2.28603939   -0.00808607    4.22064158
 O            0.04508506    0.01034939    4.14111326
 H            0.16626528    0.00902708    5.10791982
 C           -1.31965119   -0.00362401   -0.70999847
 O           -2.37888722   -0.01224081   -0.11245547
 O           -1.20544426   -0.00393627   -2.02681175
 H           -2.13735045    0.01686835   -2.45340918
 S           -3.99984273   -1.48710922   -3.42903713
 O           -3.50428326   -0.05433643   -3.16259230
 C           -2.71727942   -2.25920424   -4.43280633
 H           -2.94499903   -3.32069067   -4.54999135
 H           -2.72449367   -1.76638766   -5.40578531
 H           -1.75078293   -2.11841734   -3.94222620
 C           -3.71893080   -2.41246221   -1.90692902
 H           -4.30786807   -1.93165873   -1.12527316
 H           -4.05510871   -3.44010172   -2.05977104
 H           -2.65921682   -2.38467181   -1.64468677
```

Gaussian output file reporting the thermochemistry of the optimized structure including enthalpies and Gibbs free energies

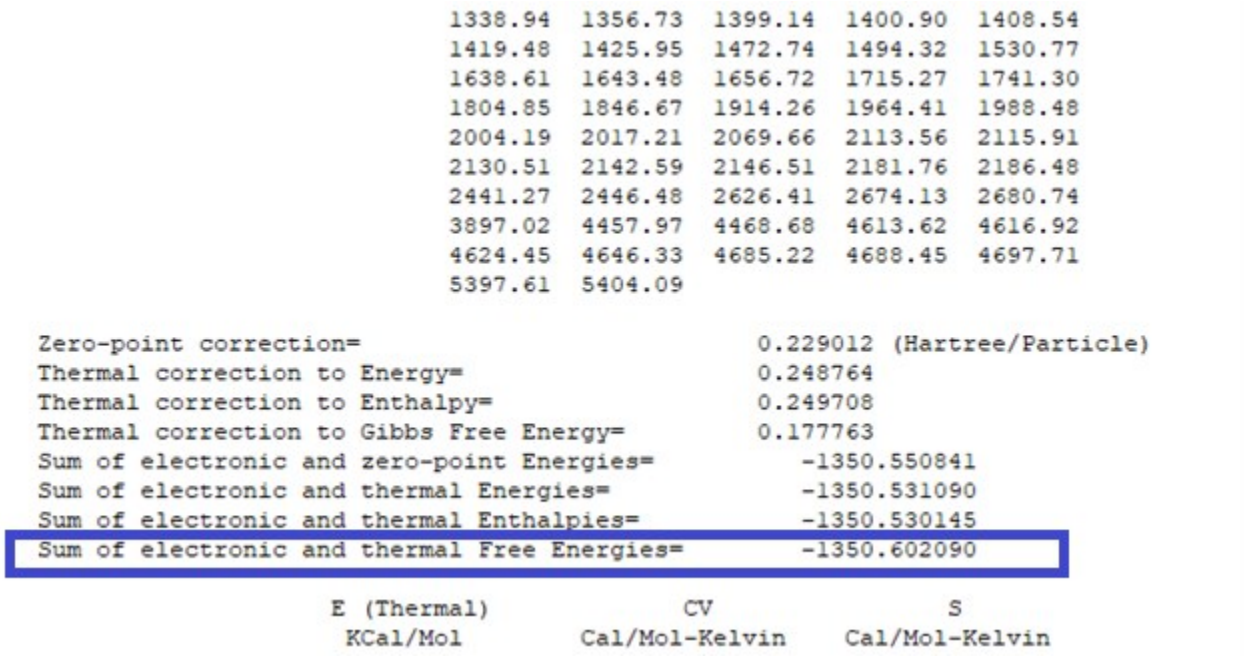

```
1338.94  1356.73  1399.14  1400.90  1408.54
1419.48  1425.95  1472.74  1494.32  1530.77
1638.61  1643.48  1656.72  1715.27  1741.30
1804.85  1846.67  1914.26  1964.41  1988.48
2004.19  2017.21  2069.66  2113.56  2115.91
2130.51  2142.59  2146.51  2181.76  2186.48
2441.27  2446.48  2626.41  2674.13  2680.74
3897.02  4457.97  4468.68  4613.62  4616.92
4624.45  4646.33  4685.22  4688.45  4697.71
5397.61  5404.09

Zero-point correction=                           0.229012 (Hartree/Particle)
Thermal correction to Energy=                    0.248764
Thermal correction to Enthalpy=                  0.249708
Thermal correction to Gibbs Free Energy=         0.177763
Sum of electronic and zero-point Energies=          -1350.550841
Sum of electronic and thermal Energies=             -1350.531090
Sum of electronic and thermal Enthalpies=           -1350.530145
Sum of electronic and thermal Free Energies=        -1350.602090

                    E (Thermal)             CV                S
                     KCal/Mol        Cal/Mol-Kelvin    Cal/Mol-Kelvin
```

References

1. Y. Zhao and D. G. Truhlar, *Theor. Chem. Acc.*, 2008, **120**, 215.
2. R. Ditchfield, W. J. Hehre and J. A. Pople, *J. Chem. Phys.* 1971, *54*, 724.
3. M. J. G. Frisch, G. W. Trucks, H. B. Schlegel, *et al*. Gaussian 09, Revision D.01 2009.
4. J. Tomasi, B. Mennucci and R. Cammi, *Chem. Rev.*, 2005, **105**, 2999.
5. V. Barone, M. Cossi and J. Tomasi, *J. Chem. Phys.*, 1997, **107**, 3210.
6. A. Rochefort, S. P. Bedwani and A. Lopez-Bezanilla, *J. Phys. Chem. C*, 2011, **115**, 18625.
7. A. Mahmood, M. Saeed, Y. Chan, A. S. Saleemi, J. Guo and S. L. Lee, *Langmuir*, 2019, **35**, 8031.
8. M. Saeed, A. Mahmood, A. S. Saleemi, X. Zeng and S. L. Lee, *J. Phys. Chem. C*, 2020, **124**, 829.
9. W. M. Haynes, Handbook of Chemistry and Physics (92nd ed.). Boca Raton, FL: *CRC Press*. 2011. ISBN 1439855110.
10. D. Aurbach, Nonaqueous Electrochemistry. *CRC Press*. 1999. ISBN 978-0824773342.